Experimental and Theoretical Studies toward a Characterization of Conceivable Intermediates Involved in the Gas-Phase Oxidation of Methane by Bare FeO^+. Generation of Four Distinguishable $[Fe,C,H_4,O]^+$ Isomers

Detlef Schröder, Andreas Fiedler, Jan Hrušák,† and Helmut Schwarz*

Contribution from the Institut für Organische Chemie, Technische Universität Berlin, W-1000 Berlin 12, F.R.G. *Received May 9, 1991*

Abstract: Sections of the potential energy surface of $[Fe,C,H_4,O]^+$ ions are probed experimentally by using collisional activation mass spectrometry as well as theoretically by ab initio MO studies. Evidence is presented for the existence of several, clearly distinguishable isomers, some of which are of relevance in the context of methane activation by FeO^+ in the gas phase. While this process initially gives rise to the formation of an encounter complex, $CH_4{\cdot}FeO^+$ (**1**), both spontaneous and post-collisional isomerization occurs to other intermediates formed from **1**. The data point to the intermediacy of CH_3–Fe–OH^+ (**3**), $CH_3O(H)Fe^+$ (**4**), and CH_2=Fe—OH_2^+ (**7**); these species account for the formation of $FeOH^+$, Fe^+, and $FeCH_2^+$, respectively. The isomers CH_3–Fe–OH^+ (**3**), $CH_3O(H)Fe^+$ (**4**), and CH_2=Fe—OH_2^+ (**7**) can be generated in a clean fashion using appropriate ion/molecule reactions in the gas phase. **4** results by termolecular association of CH_3OH and Fe^+ as well as decarbonylation of $HCOOCH_3$, **7** is formed in a termolecular reaction from H_2O and $FeCH_2^+$, and **3** is accessible by SO_2 loss from the Fe^+ complex of CH_3SO_2OH. Mixtures of **3** and **7** are obtained by the Fe^+-mediated losses of C_2H_4 from n-C_3H_7OH and decarbonylation of $HCOCH_2OH$ and CH_3COOH, pointing to a relatively complex potential energy surface of these systems. No experimental evidence has yet been obtained for the existence of the insertion products H_3CO–Fe–H^+ (**8**) and H–Fe–CH_2OH^+ (**9**) as stable gas-phase species. The former, generated initially by decarbonylation of $HCOOCH_3$, undergoes facile isomerization to $H_3CO(H)Fe^+$ (**4**), and the latter, when generated by decarbonylation of $HCOCH_2OH$, isomerizes to a 1:4 mixture of H_3C–Fe–OH^+ (**3**) and H_2C=Fe—OH_2^+ (**7**). Some of the experimentally probed isomers were further characterized by means of ab initio MO calculations using the MP2/ECP-DZ level of theory, and the computed structural features were found to correlate with the experimental results. The order of stabilities are discussed and compared, where possible, with existing or estimated thermochemical data.

Introduction

The transition-metal-mediated activation of methane is the most important of all C–H bond activation processes,[1] and, according to Barton, the problem of selective activation of alkanes constitutes the "search for the chemists' Holy Grail". This is due not only to the great economic interest in the direct conversion of alkanes to "valuable" products, but also to the inherent scientific challenge, which still remains to be met as far as the mechanistic details of the various processes are concerned. With regard to methane activation, the approach used successfully for numerous organic substrates, namely, to obtain information on the detailed steps of the activation of CH/CC bonds by "bare" transition-metal ions,[2] has failed for the simple reason that the oxidative additions of many ground-state metal ions M^+ (M = Ti, V, Co, Fe, Nb, Rh, Sc, Y, La, Lu, Co, Ni, Zn, and U)[3] to CH_4 (eq 1) is endothermic.

$$CH_4 + M^+ \rightarrow H\text{–}M\text{–}CH_3^+ \qquad \Delta H_r^\circ > 0 \qquad (1)$$

Exceptions are the transition-metal ions M^+ (M = Ta, W, Os, Ir, and Pt), which were shown recently to dehydrogenate methane.[4] Alternatively, oxidative addition can be brought about in those cases where either M^+ is electronically excited (e.g., Ti^{+5} or Cr^{+6}) or the barrier to the insertion is overcome by translationally exciting M^+.[2g,7] The reactions of "naked" metal atoms M (M = Mn, Fe, Co, Ni, Zn) with CH_4 in a noble-gas matrix are also only possible after photochemical excitation of M.[8] The often useful approach of activating CH/CC bonds not by atomic metal ions but rather by homo- or heteronuclear ionic clusters[9] has also proved fruitless.[10]

A conceivable way of favorably influencing the reaction enthalpy for activation of alkanes is the use of ionic transition-metal oxides, MO^+, instead of M^+.[11] Indeed, with regard to methane activation by FeO^+, we were recently able to demonstrate[12] that—in contrast to an earlier report[11a]—under ICR conditions the reactions shown in eq 2 take place with $k_1 = 2 \times 10^{-10}$ cm^3 molecule^{-1} s^{-1}. Although this value is smaller than that for the analogous reaction of FeO^+ with C_2H_6 ($k = 8.4 \times 10^{-10}$ cm^3

				ΔH_r° (kcal/mol)	
$FeO^+ + CH_4$	$\xrightarrow{k_1}$	0.57	$FeOH^+ + CH_3^\bullet$	−2	(2)
		0.02	$FeCH_2^+ + H_2O$	−21	
		0.41	$Fe^+ + CH_3OH$	−7	

† Permanent address: Institute of Macromolecular Chemistry, Czechoslovak Academy of Sciences, Heyrovsky Sq. 2, CS-16202 Prague, Czechoslovakia.

(1) (a) Shilov, A. E. *Activation of Saturated Hydrocarbons by Transition Metal Complexes*; D. Reidel: Boston, 1984. (b) Gesser, H. D.; Hunter, N. R.; Prakash, C. B. *Chem. Rev.* **1985**, *85*, 235. (c) Dalton, H.; Leak, D. J. In *Mechanistic Studies on the Mode of Action of Methane Monoxygenase*; Degan, H., Ed.; D. Reidel: Dordrecht, 1985; p 169. (d) Holm, R. H. *Chem. Rev.* **1987**, *87*, 1401. (e) Hill, C. L. Ed., *Activation and Functionalization of Alkanes*; Wiley: New York, 1989. (f) Davies, J. A.; Watson, P. L.; Liebman, J. F.; Greenberg, A. *Selective Hydrocarbon Activation*; VCH Publishers: New York, 1990. (g) Barton, D. H. R. *Aldrichima Acta* **1990**, *23*, 3. (h) Schwarz, H. *Angew. Chem., Int. Ed. Engl.* **1991**, *30*, 820.

(2) For recent reviews, see: (a) Freiser, B. S. *Talanta* **1985**, *32*, 697. (b) Allison, J. *Prog. Inorg. Chem.* **1986**, *34*, 627. (c) Armentrout, P. B. In *Structure/Reactivity and Thermochemistry of Ions*: Ausloos, P., Lias, S. G., Eds.; D. Reidel: Dordrecht, 1987; No. 193, p 97. (d) Ridge, D. P. *Ibid.* 1987; No. 193, p 165. (e) Russell, D. H., Ed.; *Gas Phase Inorganic Chemistry*; Plenum: New York, 1989. (f) Schwarz, H. *Acc. Chem. Res.* **1989**, *22*, 282. (g) Armentrout, P. B.; Beauchamp, J. L. *Ibid.* **1989**, *22*, 315. (h) Schwarz, H.; Eller, K. *Chimia* **1989**, *43*, 371. (i) Eller, K.; Karrass, S.; Schwarz, H. *Ber. Bunsenges. Phys. Chem.* **1990**, *94*, 1201. (j) Eller, K.; Schwarz, H. *Chem. Rev.* **1991**, *91*, 1121.

(3) Selected references: (a) Aristov, N.; Armentrout, P. B. *J. Phys. Chem.* **1987**, *91*, 6178. (b) Tonkyn, R.; Ronan, M.; Weisshaar, J. C. *Ibid.* **1988**, *92*, 92. (c) Sunderlin, L. S.; Armentrout, P. B. *J. Am. Chem. Soc.* **1989**, *111*, 3845. (d) Eller, K. Ph.D. Thesis, Technische Universität Berlin, D83, 1991.

(4) (a) Irikura, K. K.; Beauchamp, J. L. *J. Am. Chem. Soc.* **1991**, *113*, 2769. Also, see: (b) Buckner, S. W.; MacMahon, T. J.; Byrd, G. D.; Freiser, B. S. *Inorg. Chem.* **1989**, *28*, 3511. (c) Irikura, K. K.; Beauchamp, J. L. *J. Am. Chem. Soc.* **1989**, *111*, 75.

(5) Sunderlin, L. S.; Armentrout, P. B. *J. Phys. Chem.* **1988**, *92*, 1209.

(6) (a) Halle, L. F.; Armentrout, P. B.; Beauchamp, J. L. *J. Am. Chem. Soc.* **1981**, *103*, 962. (b) Reents, W. D., Jr.; Strobel, F.; Freas, R. G., III; Wronka, J.; Ridge, D. P. *J. Phys. Chem.* **1985**, *89*, 5666. (c) Georgiadis, R.; Armentrout, P. B. *Ibid.* **1988**, *92*, 7060.

(7) Schultz, R. H.; Elkind, J. L.; Armentrout, P. B. *J. Am. Chem. Soc.* **1988**, *110*, 411.

0002-7863/92/1514-1215$03.00/0

Scheme I

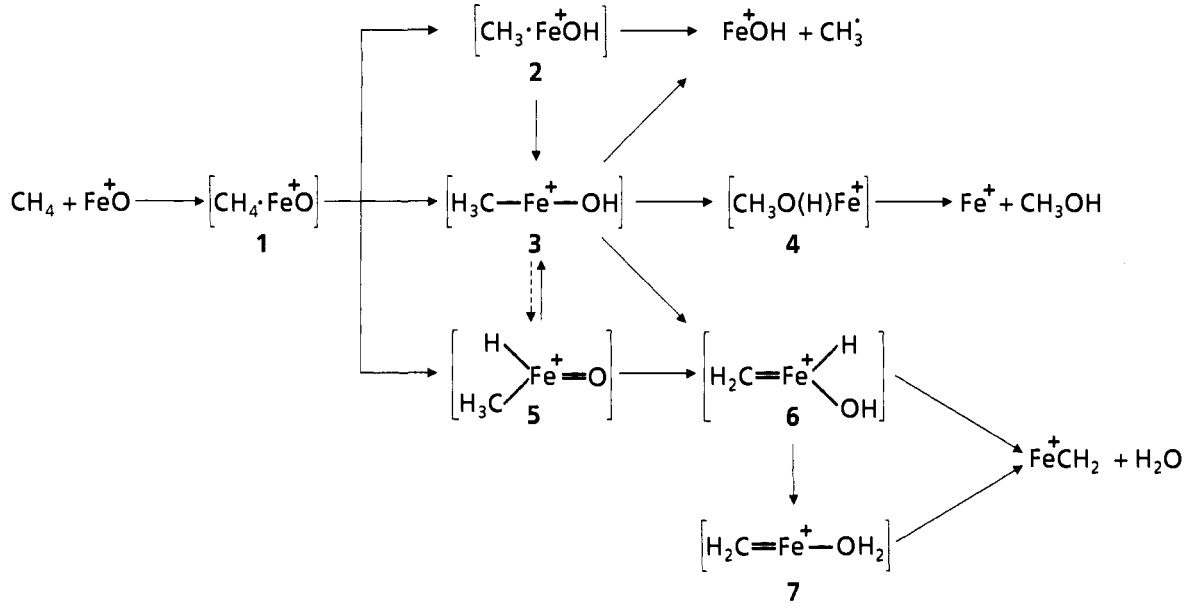

molecule^{-1} s^{-1}),[11a,13] it is still two orders of magnitude greater than the rate constants for associative reactions of M^+ with CH_4.[3b]

Although the study of the reactions of FeO^+ with CH_2D_2 and CD_4 allowed the determination of the operation of a kinetic isotope effect ($k_H/k_D = 4.6$) in the CH/CD activation step,[12] the actual intermediates generated in the course of eq. 2 remained unknown. In fact, despite the power of the ICR technique to identify reaction partners, to determine the rates of gas-phase ion/molecule reactions, to exert some control on the energetics of the process by translationally exciting ionic substrates, and to structurally identify the ionic reaction products by means of further ion/molecule processes or collision-induced dissociations, the unambiguous identification of *reactive intermediates* ("transients") by using ICR is, on principal grounds, difficult if not impossible at all.[14] Consequently, different techniques have to be employed in order to solve this fundamental problem.

With regard to methane activation by FeO^+, it is not unreasonable to suggest that—among other species—the intermediates depicted in Scheme I may be formed en route to the products. However, the $[Fe,C,H_4,O]^+$ ions shown in Scheme I do by no means represent a complete set of possible isomers. Additional isomers, which are plausible from a chemical point of view, may include H_3CO–Fe–H^+ (**8**) H–Fe–CH_2OH^+ (**9**). The central problem we will be addressing concerns the question: which $[Fe,C,H_4,O]^+$ isomers exist in potential wells deep enough to probe the isomers by means of tandem mass spectrometric techniques?

Valuable structural information on gaseous ions residing in potential wells is experimentally available by generating the ions in the presence of an inert buffer gas, mass-selecting the species of interest in a beam experiment, and subjecting it to a high-energy collision experiment. As repeatedly demonstrated,[15] the so-obtained collisional activation (CA) mass spectra do not only serve as a fingerprint to distinguish isomeric ions; quite often, and in particular for smaller systems, the CA mass spectra contain structure-indicative signals which can be used to infer the connectivity of the ions. Of course, detailed structural information beyond cross-structural features is not available by using this relatively straight-forward mass-spectrometric technique. In addition, the possibility of post-collisional isomerization cannot be ignored. This holds true, in particular, for those isomers residing in relatively shallow potential wells.

An alternative, quite powerful approach to structurally characterize isolated ions takes advantage of high-level ab initio MO studies which, nowadays, can be performed routinely for small-sized *organic* systems with an accuracy of better than ±2 kcal/mol.[16] However, in the case of transition-metal compounds, the increasing number of electrons, the proper treatment of relativistic effects, and the almost degenerate electronic states dramatically limit the size of the system if one aims at an accuracy typical for the pure organic species.[17] This situation is indeed problematic, as, for transition-metal-containing systems of chemical relevance (as, for example, the species described in the present study), the application of an all-electron formalism suggests for practical purposes the use of small basis sets, although it is well-known that even after the inclusion of polarization functions the description of geometic and energetic features often remain poor.[18] For medium-sized systems the application of the "frozen core" approximation has been suggested repeatedly, and, as recently reviewed,[19] various effective core and/or pseudo-potential algorithms have been developed and successfully applied to the study of transition-metal complexes.

Here we will demonstrate by using collisional activation mass spectrometry that at least four distinguishable isomers of the elemental composition $[Fe,C,H_4,O]^+$ exist in the gas phase. Experimental evidence will be presented for the formation of **1**,

(8) (a) Ozin, G. A.; McCaffrey, J. G.; McIntosh, D. F. *Pure Appl. Chem.* **1984**, *56*, 111. (b) Kafafi, Z. H.; Hauge, R. H.; Margrave, J. L. *J. Am. Chem. Soc.* **1985**, *107*, 6134. (c) Kafafi, Z. H. In ref 1f, Chapter 12, and references cited therein. (d) For matrix experiments on photoinduced CH_4 activation of transition-metal fragments, see: Perutz, R. N. *Pure Appl. Chem.* **1990**, *62*, 1103.

(9) (a) Buckner, S. W.; Freiser, B. S. *Polyhedron* **1988**, *7*, 1583. (b) Freiser, B. S. *Chemtracts: Anal. Phys. Chem.* **1989**, *1*, 65.

(10) (a) Huang, Y.; Freiser, B. S. *J. Am. Chem. Soc.* **1988**, *110*, 387. (b) Irion, M. P.; Selinger, A. *Ber. Bunsenges. Phys. Chem.* **1989**, *93*, 1408.

(11) (a) Jackson, T. C.; Jacobson, D. B.; Freiser, B. S. *J. Am. Chem. Soc.* **1984**, *106*, 1252. (b) See also ref 4c.

(12) Schröder, D.; Schwarz, H. *Angew. Chem., Int. Ed. Engl.* **1990**, *29*, 1433.

(13) Schröder, D.; Schwarz, H. *Angew. Chem., Int. Ed. Engl.* **1990**, *29*, 1431.

(14) For a recent review on the strengths and drawbacks of ICR, see: Nibbering, N. M. M. *Acc. Chem. Res.* **1990**, *23*, 279, and references therein.

(15) (a) Levsen, K.; Schwarz, H. *Angew. Chem., Int. Ed. Engl.* **1976**, *15*, 509. (b) Cooks, R. G., Ed. *Collision Spectroscopy*; Plenum: New York, 1978. (c) McLafferty, F. W., Ed. *Tandem Mass Spectrometry*; Wiley Interscience: New York, 1983. (d) Levsen, K.; Schwarz, H. *Mass Spectrom. Rev.* **1985**, *3*, 77. (e) Bordas-Nagy, J.; Jennings, K. R. *Int. J. Mass Spectrom. Ion Processes* **1990**, *100*, 105.

(16) Pople, J. A.; Head-Gordon, M.; Fox, D. J.; Raghavachari, K.; Curtiss, L. A. *J. Chem. Phys.* **1989**, *90*, 5622.

(17) Lüthi, H. P.; Ammeter, J. H.; Almlöf, J.; Faegri, K., Jr. *J. Chem. Phys.* **1982**, *77*, 2002.

(18) Swanstrom, P.; Jorgensen, K. A. *J. Chem. Soc., Dalton Trans.* **1990**, 1155.

(19) (a) Langhoff, S. R.; Bauschlicher, C. W., Jr. *Annu. Rev. Phys. Chem.* **1988**, *39*, 181. (b) Tsipis, C. A. *Coord. Chem. Rev.* **1991**, *108*, 163.

3, 4, and 7. The characterization of the other species is less certain. In fact, the isomers 8 and 9 are not stable under the experimental conditions employed to generate them from the precursors used; rather they isomerize to mixtures having varying amounts of 3 and 7. The interpretation of the experimental results is aided by ab initio MP2/ECP-DZ MO calculations. These do not only provide relative stabilities of the localized minima; in addition, helpful indications are provided that some species do not seem to play a role on the potential energy surface of $[Fe,C,H_4,O]^+$ isomers. For example, all attempts to locate the ion/dipole complex $[CH_3{\cdot}FeOH]^+$ (2), which might be viewed as emerging from the encounter complex 1[20] by a hydrogen transfer, failed. As will be discussed later, geometry optimization invariably leads to $H_3C{-}Fe{-}OH^+$ (3). Similarly, attempts to localize the CH-insertion product of FeO^+ into CH_4 failed (Scheme I; 1 → 5); rather, 3 results as insertion product, and the preference to form 3 seems to be a direct corollary of the particular geometric structure of $CH_4{-}FeO^+$ (1).

Experimental and Theoretical Section

The experimental set-up has been described in earlier papers. Briefly, a 1:5–10 mixture of $Fe(CO)_5$ and suitable organic substrates is bombarded with 100-eV electrons in the chemical ionization source (repeller voltage ca. 0 V) of a substantially modified ZAB mass spectrometer of BEBE configuration (B stands for magnetic and E for electrostatic section).[21] Although the actual mechanisms by which the $[Fe,C,H_4,O]^+$ species are generated is yet unknown, the pressure in the ion source is high enough to permit collisional cooling of the organometallic complexes formed. Collision-induced dissociations were brought about by mass-selecting a beam of 8-keV kinetic energy having the elemental composition $[Fe,C,H_4,O]^+$ by means of B(1)E(1) at a resolution sufficiently high to separate isobaric multiplets. This beam is collided with helium as a stationary gas (80% transmission; this corresponds, on the average, to 1.1–1.2 collisions[22]). Ionic dissociation products were recorded by scanning B(2). The second electrostatic analyzer E(2) of the machine is not used in the present experiments. Signal-averaging techniques were employed to improve the S/N ratio. Between 20 and 50 scans were accumulated by on-line processing the data with the VG 11/250 or the AMD-Intectra data system. For H/D exchange experiments, the ion source and the inlet system were flooded for 4 h with D_2O vapor (>99% deuterium). The organic compounds used were either commercially available in high purity and employed without further purification or synthesized by standard laboratory procedures.

All calculations were carried out using the GAUSSIAN 88 program package.[23] The double-zeta (DZ) basis of Dunning and Huzinaga was used for carbon, oxygen, and hydrogen atoms.[24] The core electrons of iron were fit to an effective core potential (ECP), while the valence electrons were described by a DZ basis.[25] This basis set will be referred to as ECP-DZ and, as shown previously,[26] it allows a satisfying description of both excitation and ionization energies for the low-lying electronic states of iron. In order to account for electron-correlation effects, post-SCF calculations based on second-order Møller–Plesset perturbation theory (MP2)[27] were performed. The geometries of the systems were fully optimized at the SCF level by using standard gradient techniques; no restrictions resulting from symmetry constraints were used. The charge distributions were calculated by a Mulliken population analysis. The energies given refer to the lowest found configurations which, at the UHF level, correspond to the *sextet* states. We have also calculated the lowest quartet states; although the quartet states also correspond to minima, they were invariably found to be much higher in energy; consequently, they are omitted from the discussion. Date are available upon request from the authors. In order to estimate the contamination by higher spin multiplicities, the calculated expectation values, $\langle S^2 \rangle$, were computed. It was found that contributions of higher states amount to less than 1%.

As the primary objective of the theoretical study was aimed at locating possible minima on the $[Fe,C,H_4,O]^+$ potential energy surface and to provide an explanation for the experimental findings, we did not use the much more sophisticated multi-reference approach. While such an approach will undoubtedly lead to a significant improvement of the calculated energies, the size of our system is prohibitive for this type of calculation.

Some insight concerning the reliability and performance of the levels of theory employed in the present study is provided by the data given in Tables I II. In Table I the bond dissociation energy (BDE) for the reaction $CH_3O(H)Fe^+$ (4) → $Fe^+ + CH_3OH$ is reported for three different basis sets, and corrections for the UHF energies were made by MP2 and by configuration interaction with single and double excitation (CISD). The contamination of the wave function due to higher spin contributions lies in the range of 0.2–0.6%, relative to the expectation value for a pure sextet state. As can be seen by a comparison of the calculated BDE with the experimental figures, the latter varying between 27 and 40 kcal/mol,[28] the two minimal basis sets STO-3G* and ECP-MP lead to a severe overestimation of BDE. In contrast, the ECP-DZ basis yields a much smaller stabilization energy for the $CH_3O(H)Fe^+$ complex 4. We suppose that, after correction for the basis set superposition error, a further drop by ca. 5 kcal/mol is realistic,[29] thus bringing our calculated BDE quite close to the experimental figure. Interestingly, post-SCF corrections on the UHF geometries have no substantial effects on the BDE of $(CH_3OH)Fe^+$.

In order to estimate further the suitability of our "best" method to predict relative energies of the various $[Fe,C,H_4,O]^+$ isomers of interest to be discussed later, a comparison was made with thermochemical data where these are available. As demonstrated in Table II, the agreement is, except for the notorious case of $FeCH_2^+$,[30] better than 10 kcal/mol. The deviation of the multiply bonded system $FeCH_2^+$ is a general feature of the single-determinant approach used.[26]

Table I. Comparison of the Calculated Bond Dissociation Energy (BDE) for the Process $CH_3O(H)Fe^{+\cdot}$ (4) → $CH_3OH + Fe^{+\,a,b}$

	UHF/UHF	MP2/UHF	CISD/UHF
STO-3G*	79	90	88
ECP-MP	66	73	71
ECP-DZ	46	50	49

[a] Data are given in kcal/mol. [b] The experimentally determined BDE varies between 27 and 40 kcal/mol (see ref 28).

Table II. Experimental and Calculated Thermochemical Data, $\Delta H_f°$, for Some Fragmentation Reactions of $[Fe,C,H_4,O]^+$ Ions

	$\Delta H_f°$(exp)[b]	$\Delta H_f°$(calc)[c]
$Fe^+ + CH_3OH$	237	(237)
$FeOH^+ + CH_3^\cdot$	246	246
$FeCH_3^+ + OH^\cdot$	266	262
$FeCH_2^+ + H_2O$	234	268
$FeOH_2^+ + CH_2$	287[b,d]	285
$FeO^+ + CH_4$	247	256

[a] Data are given in kcal/mol. [b] Taken from ref 31. [c] $\Delta H_f°$ were calculated from the relative stabilities obtained at the ECP-DZ level of theory using separated Fe^+/CH_3OH as a reference and setting the calculated figure of this system equal to 237 kcal/mol. [d] Estimated from data given in ref 32.

Results and Discussion

Inspection of the CA mass spectra (Table III) of the $[Fe,C,H_4,O]^+$ ions generated from the systems I to VIII demonstrate

(20) For the characterization of the ion-induced dipole bond complex $Fe^{+\cdot}{\cdot}C_3H_8$, see: Schultz, R. H.; Armentrout, P. B. *J. Am. Chem. Soc.* **1991**, *113*, 729.

(21) Actually, our four-sector mass spectrometer consists of two double-focusing units: MS-I is the BE part of an original ZAB-3F machine and MS-II is an AMD 604 mass spectrometer. For a detailed description, see: (a) Srinivas, R.; Sülzle, D.; Koch, W.; DePuy, C. H.; Schwarz, H. *J. Am. Chem. Soc.* **1991**, *113*, 5970. (b) Srinivas, R.; Sülzle, D.; Weiske, T.; Schwarz, H. *Int. J. Mass Spectrom. Ion Processes* **1990**, *107*, 369.

(22) Holmes, J. L. *Org. Mass Spectrom.* **1985**, *20*, 169.

(23) Frisch, M. J.; Head-Gordon, M.; Schlegel, H. B.; Raghavachari, K.; Binkley, J. S.; Gonzales, C.; Defrees, D. J.; Fox, D. J.; Whiteside, R. A.; Seeger, R.; Melius, C. F.; Baker, J.; Martin, R. L.; Kahn, L. R.; Stewart, J. J. P.; Fluder, E. M.; Toplol, S., Pople, J. A. Gaussian, Inc., Pittsburgh PA.

(24) Dunning, T. H.; Hay, P. J. *Modern Theoretical Chemistry*; Plenum: New York, 1976; p 1.

(25) Hay, P. J.; Wadt, W. R. *J. Chem. Phys.* **1985**, *82*, 270.

(26) McKee, M. L. *J. Am. Chem. Soc.* **1990**, *112*, 2601.

(27) Møller, C.; Plesset, M. S. *Phys. Rev.* **1934**, *46*, 618.

(28) Allison, J.; Ridge, D. P. *J. Am. Chem. Soc.* **1979**, *101*, 4998.

(29) Sakaki, S.; Koga, N.; Morokuma, K. *Inorg. Chem.* **1990**, *29*, 3110.

(30) For a detailed discussion, see: (a) ref 26. (b) Veldkamp, A., Diploma Thesis, Universität Marburg, 1991. (c) Veldkamp, A.; Frenking, G. *J. Chem. Soc., Chem. Commun.*, in press. We are grateful to Professor Gernot Frenking, Marburg, for having provided us with a copy of the unpublished results from the thesis of A. Veldkamp.

(31) Lias, S. G.; Bartmess, J. D.; Liebmann, J. F.; Holmes, J. L.; Levin, R. D.; Mallard, W. G. *J. Phys. Chem. Ref. Data* **1988**, *17*, Suppl. 1.

(32) Maguera, T. F.; David, D. E.; Michl, J. *J. Am. Chem. Soc.* **1989**, *111*, 4100.

Table III. Collisional Activation (CA) Mass Spectra of $[Fe,C,H_4,O]^+$ Isomers[a]

		$Fe(CO)_5$ and organic precursor							
Δm	composition of ionic product	c-C_3H_6/H_2O I	CH_3SO_2OH II	CH_3OH III	$HCOOCH_3$ IV	CH_4/N_2O V	n-C_3H_7OH VI	$HCOCH_2OH$ VII	CH_3COOH VIII
1		7	<1	4	4	1	2	1	6
2		5	<1	1	1		1	1	4
14	$FeOH_2^+$	25	<1	≪1	≪1	1	2	2	20
15	$FeOH^+$	6	100	50	60	20	100	100	30
16	FeO^+	<1	4	2	2	100	4	3	2
17	$FeCH_3^+$	≪1	9	<1	<1	1	8	8	4
18	$FeCH_2^+$	100	4	<1	<1	15	13	25	100
19	$FeCH^+$	20	3	<1	<1	1	4	6	20
20	FeC^+	10	2	<1	<1		3	2	10
31	FeH^+	2	3	9	12	2	5	3	2
32	Fe^+	15	35	100	100	50	50	50	25
56	$CH_3OH^{\cdot+}$			<1	<1				
57	CH_2OH^+	≪1	≪1	1	1		≪1	≪1	≪1
	structure assign	**7**	**3**	**4**	**4**	**1, 3, 4, 7**	**3 + 7** (10:1)	**3 + 7** (5:1)	**3 + 7** (1:4)

[a] Data are given in % base peak.

Table IV. CA Mass Spectra of $[Fe,C,H_{4-x},D_x,O]^+$ Isotopomers[a]

	$Fe(CO)_5$ and deuterated precursor						
Δm	c-C_3H_6/D_2O Ia	CH_3SO_2OD IIa	CD_3OH IIIa	$HCOOCD_3$ IVa	CD_4/N_2O Va	$CD_3CH_2CH_2OH$ VIa	CD_3COOH VIIIa
1	10	<1	3	4		<1	<1
2	7	<1	1	1	1	2	3
3	≪1	<1	1	1		1	<1
4	≪1	<1	<1	<1		<1	3
14	25	<1					
15		100					<1
16	4	<1	<1	<1	2	2	15
17		2	1	2		15	6
18	≪1	8	35	50	30	100	20
19	≪1	4	2	4		10	100
20	100	3			100	<1	2
21	20	2	<1	<1		4	10
22	10				2		<1
23			<1	<1		3	6
FeD^+	1	1	5	5	4	4	3
FeH^+	1	1	1	2		1	1
Fe^+	20	35	100	100	30	40	30

[a] Data are given in % base peak.

Scheme II

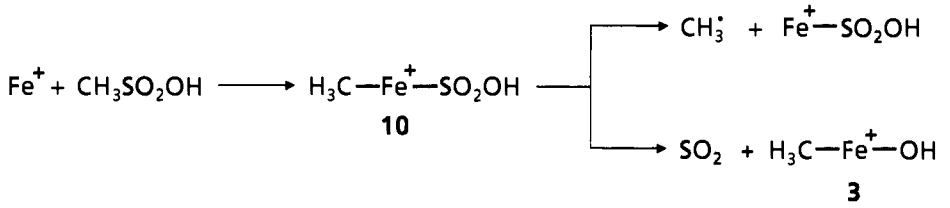

that several distinguishable isomers exist, which have lifetimes exceeding 10^{-5} s. As already mentioned, clearly assignable ionic products are found in systems I, II, III, and IV which give rise to the novel organometallic ions $CH_2{=}F{-}OH_2^+$ (**7**), $CH_3{-}Fe{-}OH^+$ (**3**) and $CH_3O(H)Fe^+$ (**4**), respectively. The organization of this section is such that each system will be discussed separately. Where appropriate, we will also refer to the labeling results (Table IV).[33] The theoretical findings will be discussed separately at the end.

(1) System I. As previously reported,[34] the reaction of Fe^+ with c-C_3H_6 gives rise to the formation of $FeCH_2^+$, which in the presence of water is trapped as $CH_2{=}Fe{-}OH_2^+$ (**7**). In fact, the connectivity of this ion is directly reflected in its CA mass spectrum exhibiting as the major processes the losses of H_2O ($\rightarrow FeCH_2^+$: 100%) and of CH_2 ($\rightarrow Fe(OH_2)^+$: 25%). Further support for this assignment is provided by the CA mass spectrum of $CH_2{=}Fe{-}(OD_2)^+$ (**7a**). The latter is generated from the system $Fe(CO)_5/c\text{-}C_3H_6/D_2O$. We note from Table IV the specific losses of $\Delta m = 20$, D_2O (100%) and of $\Delta m = 14$, CH_2 (25%). This finding not only substantiates our proposal for the genesis of $CH_2{=}Fe{-}OD_2^+$ (**7a**), but, in addition, it demonstrates that no (if any) substantial hydrogen exchange between the two ligands of **7a** is operative.[35] We also note from Table III that the formations of $FeCH^+$ and FeC^+ (possibly by further disso-

(33) The relative intensity differences between the CA mass spectra of labeled and unlabeled species (Tables III and IV) originate mostly from the introduction of the deuterium. The variation of conditions of the ion source is of minor importance.

(34) Jacobson, D. D.; Freiser, B. S. *Organometallics* **1990**, *9*, 1493.

(35) It is quite interesting to recall that in the reaction of *neutral* $FeCH_2$ with H_2O in argon matrices the only observable product corresponds to the formation of $HOFeCH_3$. This distinct behavior either reflects an inherently different chemistry of $FeCH_2$ and $FeCH_2^+$ or—less likely—is due to the particular conditions prevailing in the matrix experiment.

Scheme III

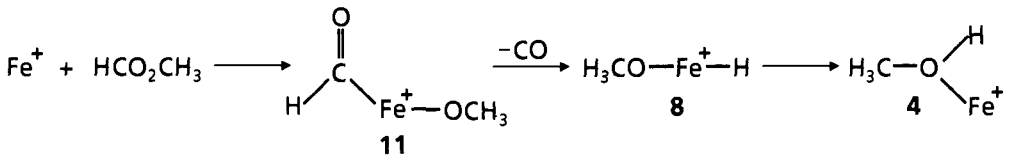

ciation of $FeCH_2^+$) are—in comparison to the other systems—quite pronounced.

(2) System II. In both the metastable ion and the CA mass spectra of the complex CH_3SO_2OH/Fe^+ (system II), the dominant reactions are due to the losses of $CH_3^\bullet$ and SO_2. Elimination of a methyl radical is indicative for insertion of Fe^+ in the C–S bond. This insertion intermediate **10** may also serve as a precursor to generate, upon SO_2 elimination, the ion CH_3–Fe–OH^+ (**3**) (Scheme II). Formally, ion **3** corresponds to the insertion of Fe^+ into the C–O bond of methanol.

Our assignment for **3** is based on the CA spectrum (Table III) and the experiment conducted with CH_3SO_2OD (Table IV). We note that the dominant collision-induced dissociation of **3** corresponds to the loss of Δm = 15, $CH_3^\bullet$ (100%); in line with existing thermochemical data,[31,36] this reaction is by at least 20 kcal/mol favored when compared with the loss of the more strongly bound $OH^\bullet$ radical ($\Delta H_f^\circ(FeOH^+ + CH_3^\bullet)$ = 246 kcal/mol; ΔH_f° ($FeCH_3^+ + OH$) = 266 kcal/mol). The CA mass spectrum of the isotopomer CH_3–Fe–OD^+, **3a**, generated from $Fe(CO)_5/CH_3SO_2OD$, exhibits the specific elimination of Δm = 15 (100%), and the hydroxyl radical eliminated largely contains the deuterium atom. In distinct contrast to the isomer CH_2=Fe–OH_2^+ (**7**), collisional activation of CH_3–Fe–OH^+ (**3**) does not give rise to any significant losses of CH_2, and/or H_2O. Consequently, and in line with the deuterium-labeling experiments, the isomers **3** and **7** do not interconvert on the time scale available to the system (ca. 1 μs).

(3) Systems III and IV. The CA mass spectra of the $[Fe,C,H_4,O]^+$ isomers generated from III ($Fe(CO)_5/CH_3OH$) and IV ($Fe(CO)_5/HCOOCH_3$) are very similar to each other and quite distinct from the CA spectra of CH_3–Fe–OH^+ (**3**) and CH_2=Fe–OH_2^+ (**7**). In the CA spectra of the ions in systems III and IV, the dominant reactions are due to the loss of CH_3OH (→Fe^+: 100%) and the elimination of $CH_3^\bullet$ (→$FeOH^+$: 50%). We also observe, though weak, a structure-indicative signal at m/z 32 ($CH_3OH^{+\bullet}$), which is absent in the CA mass spectra of all other $[Fe,C,H_4,O]^+$ isomers. In the isotopomers generated from $Fe(CO)_5/CD_3OH$ or $Fe(CO)_5/HCO_2CD_3$, the weak methanol$^{+\bullet}$ signal m/z 32 is shifted to m/z 35, $CD_3OH^{+\bullet}$ (not given in Table IV), and the methyl radical lost contains three deuterium atoms (Δm = 18). These findings are compatible with the formation of the ion/molecule complex $CH_3O(H)Fe^+$ (**4**), in which the intact methanol molecule serves as a ligand. Insertion of Fe^+ into the C–O bond (i.e., structure CH_3–Fe–OH^+ (**3**) is less likely on the ground that in the CA spectrum of systems III and IV (in contrast to I and II), signals indicative for the $FeCH_x^+$ unit (x = 0–3) are of very low intensity. From the near-identity of the CA spectra for the systems III and IV (Table III), we propose that in the course of Fe^+-mediated decarbonylation of $HCOOCH_3$ the intermediate H–Fe–OCH_3^+ (**8**) undergoes rapid isomerization to **4** (Scheme III). The origin of the facile rearrangement of the formally O–H insertion product **8** to the ion/molecule complex **4** remains to be elucidated and can—as suggested by a reviewer—result from post-collisional isomerization. In fact, as indicated by the ab initio MO studies (see below), ion **8**, though being a genuine minimum on the potential energy surface of $[Fe,C,H_4,O]^+$, is ca. 50 kcal/mol less stable than the $Fe(CH_3OH)^+$ complex **4**. Less likely, although not impossible, is the alternative that decarbonylation of **11** will not initially generate **8** but rather, in a complex multicenter process, **11** directly decomposes to **4**.

(36) (a) Armentrout, P. B.; Georgiadis, R. *Polyhedron* **1988**, *7*, 1573. (b) Reference 2g. (c) Martinho Simões, J. A.; Beauchamp, J. L. *Chem. Rev.* **1990**, *90*, 629.

(4) System V. As demonstrated earlier,[37] FeO^+ is conveniently generated from N_2O and Fe^+. In the presence of excess of CH_4, FeO^+ and CH_4 give rise to an ion having the elemental composition $[Fe,C,H_4,O]^+$. While under ICR conditions, this "encounter" complex is not observed but rather decomposes to the products given in eq 2, the pressure prevailing in the chemical ionization (CI) source of our BEBE machine brings about collisional stabilization such that a "long-lived" $[Fe,C,H_4,O]^+$ ion can be extracted from the CI source. The CA mass spectrum of this ion is given in Table III (system V). This spectrum is distinctly different from the spectra obtained for the systems I–IV, and as the spectrum cannot be reproduced by linear combinations of the CA spectra of systems I–IV, we conclude that the ionic species generated in the reaction of FeO^+ with CH_4 (system V) must contain at least one additional isomer being different from **3**, **4**, and **7**. Obviously, the presence of a very intense signal for FeO^+ (100%), which is negligible in the CA spectra of all other $[Fe,C,H_4,O]^+$ isomers, points to a structure, which already contains the "FeO" connectivity, as in the ion/dipole complex **1**. The signal corresponding to $FeOH^+$ may have several origins: (i) collision-induced dissociation of the ion/dipole complex **1** accompanied by hydrogen transfer; (ii) post-collisional isomerization of **1** to a structurally distinct isomer **2**, followed by loss of the weakly bound methyl radical; (iii) methyl loss from the insertion product CH_3–Fe–OH^+ (**3**) which can also account for the generation of $FeOH^+$. The latter isomer, which formally corresponds to the insertion of Fe^+ in the C–O bond of CH_3OH,[42] is, in principle, accessible from **1** by a collision-induced four-center reaction (σ-metathesis process)[43] in the course of which the CH bond of CH_4 is added across the FeO^+ bond. **3** itself can, of course, account for the presence of Fe^+ in the CA spectrum of system V, as direct reductive elimination of CH_3OH from **3** or from **4** will generate Fe^+. The signal for $FeCH_2^+$ (loss of H_2O) is perhaps the result of a post-collisional isomerization of **1** leading eventually to **7**. Unfortunately, the present data do not permit the estimation of the relative contributions of the four isomers generated in the course of collisional activation of the FeO^+/CH_4 system. However, there cannot possibly exist any doubt, that **1**, **3**, **4**, and **7** play a role in the reaction of FeO^+ with CH_4.

(5) Systems VI, VII, and VIII. In an attempt to generate the C–O and the H–C insertion products of CH_3OH, e.g., CH_3–Fe–OH^+ (**3**) and H–Fe–CH_2OH^+ (**9**), we have employed as precursors *n*-C_3H_7OH (VI), $HCOCH_2OH$ (VII), and CH_3COOH (VIII). Earlier labeling studies[38] suggest that Fe^+-mediated C_2H_4 loss from $CH_3CH_2CH_2OH$ involves the α- and β-CH_2 groups of 1-propanol. Thus, it is not unreasonable to expect that CH_3–

(37) Kappes, M. M.; Staley, R. H. *J. Am. Chem. Soc.* **1981**, *103*, 1286.

(38) (a) Karrass, S.; Prüsse, T.; Eller, K.; Schwarz, H. *J. Am. Chem. Soc.* **1989**, *111*, 9018. (b) Schröder, D.; Schwarz, H, unpublished results.

(39) All energies of the $[Fe,C,H_4,O]^+$ isomers discussed in this section are given relative to separated FeO^+ and CH_4, for which we assign E = 0 kcal/mol.

(40) (a) Marinelli, P. J.; Squires, R. R. *J. Am. Chem. Soc.* **1989**, *111*, 4101. (b) Carter, E. A.; Goddard, W. A., III *J. Phys. Chem.* **1988**, *92*, 5679. (c) Rosi, M.; Bauschlicher, C. W., Jr. *J. Chem. Phys.* **1990**, *92*, 1876.

(41) For the interesting topic of O–H bond activation of ROH (R = H, alkyl) by transition-metal ions in the gas phase, see: Blum, O.; Schröder, D.; Stöckigt, D.; Schwarz, H. *Angew. Chem., Int. Ed. Engl.* submitted, and references therein.

(42) For metal-complex mediated C–O bond cleavage, see: (a) Jang, S.; Atagi, L. M.; Mayer, J. M. *J. Am. Chem. Soc.* **1990**, *112*, 6413. (b) Rondon, D.; Chandret, B.; He, X.-D.; Labrone, D. *Ibid.* **1991**, *113*, 5671.

(43) Thompson, M. E.; Baxter, S. M.; Bulls, A. R.; Burger, B. J.; Nohan, M. C.; Santarsiero, B. D.; Schaefer, W. P.; Bercaw, J. E. *J. Am. Chem. Soc.* **1987**, *109*, 203.

Table V. Electron Population at the Iron Atom As Expressed in s, p, and d Electrons for $[Fe,C,H_4,O]^+$ Isomers

		s	p		total	d			total	total
CH_4·FeO^+	**1**	0.24	0.03	0.09	0.12	1.09	2.13	3.03	6.25	6.61
H_3C–Fe–OH^+	**3**	0.22	0.05	0.11	0.16	1.17	2.14	2.92	6.23	6.61
$CH_3O(H)Fe^+$	**4**	0.96	0.10	0.02	0.12	1.20	2.10	2.74	6.04	7.12
H_2C=Fe-OH_2^+	**7**	0.44	0.05	0.07	0.12	1.09	2.03	3.03	6.15	6.71
H_3CO–Fe–H^+	**8**	0.67	0.18	0.01	0.19	1.27	2.01	2.87	6.15	7.01
H–Fe–$O(H)CH_2^+$	**14**	0.66	0.18	0.02	0.20	1.11	2.10	2.93	6.14	7.00
H–Fe–OH^+		0.67	0.17	0.00	0.17	1.37	2.01	2.77	6.15	6.99

Fe–OH^+ (**3**) is accessible by this route. Similarly, one may argue that decarbonylation of CH_3COOH also gives rise to CH_3–Fe–OH^+ (**3**), while decarbonylation of $HCOCH_2OH$ may bring about the formation of H–Fe–CH_2OH^+ (**9**). However, the analysis of the CA data for these systems (Table III) does not fully support this conjecture. In contrast, the CA data are best interpreted in terms of a mixture of ions **3** (CH_3–Fe–OH^+) and **7** (CH_2=Fe—OH_2^+). We have also considered other possible explanations without arriving at a consistent description of the data given in Tables III and IV. However, the CA spectra for the systems VI, VII, and VIII can be reproduced quite well by a linear combination of the CA spectra of CH_3–Fe–OH^+ (**3**) and CH_2=Fe—OH_2^+ (**7**) in the ratios 10:1 (system VI), 5:1 (system VII), and 1:4 (system VIII), respectively. While the C–O insertion product CH_3–Fe–OH^+ (**3**) is clearly present as a stable ion, there is no experimental support for the formation of a stable H–Fe^+–CH_2OH insertion product. As demonstrated in the Theoretical Section, this conclusion is supported by the ab initio calculations according to which **9** is not a stationary point. Decarbonylation of HCO-CH_2OH is accompanied by a complex isomerization to eventually generate a 5:1 mixture of H_3C–Fe–OH^+ (**3**) and H_2C=Fe—OH_2^+ (**7**). The mechanistic details are unknown. The interpretation, of dealing with mixtures of ions **3** and **7**, is also supported by the data for the deuterated systems VIa and VIIIa (Table IV).

In conclusion, the present data present for the first time evidence that several, experimentally distinguishable isomers exist on the $[Fe,C,H_4,O]^+$ potential energy surface. While the connectivities for the isomers CH_4FeO^+ (**1**), CH_3–Fe–OH^+ (**3**), $CH_3O(H)Fe^+$ (**4**), and CH_2=Fe—OH_2^+ (**7**) can be clearly determined using collisional activation mass spectrometry, application of this method to the $[Fe,C,H_4,O]^+$ ions generated from FeO^+/CH_4 indicates the formation of several isomers, including the ion/dipole complex CH_4·FeO^+ (**1**), the insertion product CH_3–Fe–OH^+ (**3**), the methanol/Fe^+ adduct **4**, and the high-valent complex CH_2=Fe—OH_2^+ (**7**). In addition the experiments indicate that seemingly simple processes, like the loss of C_2H_4 from *n*-C_3H_7OH or decarbonylation of $HCOCH_2OH$ or CH_3COOH in the presence of Fe^+, do not necessarily give rise to "pure" ions of the expected connectivities CH_3O–Fe–H^+ (**8**) and H–Fe–CH_2OH^+ (**9**); rather, mixtures of CH_3–Fe–OH^+ (**3**) and CH_2=Fe—OH_2^+ (**7**) are generated from these precursors, thus pointing to relatively complex potential energy surfaces. As will be demonstrated in the next section, this is due to the fact that some of the isomers, like **9**, are no minima, or that post-collisional isomerization is operative.

Calculated Structural Features and Relative Energies of $[Fe,C,H_4,O]^+$ Isomers

For the methane–iron oxide complex, which corresponds to the initially formed species in the gas-phase oxidation of CH_4 by FeO^+, we obtained the C_{3v}-symmetric structure **1**. With regard to the separated building blocks CH_4 and FeO^+, **1** is stabilized by 12 kcal/mol.[39] In the ion/dipole complex **1** three hydrogen atoms of the methane subunit point to the FeO^+ dipole; as a result, the polarity of the CH bonds increases dramatically as compared to the CH bond in neutral methane (q_H = 0.17; q_C = −0.68). In addition, the C–H bond length of the three hydrogen atoms pointing to the cationic irons are elongated by 0.01 Å as compared to the uncomplexed CH bond. The electrostatic interaction of the two building blocks brings about an elongation of the Fe–O bond length by 0.03 Å (compared with free FeO^+), and the quite long distance of 2.412 Å between the three "complexed" hydrogen atoms of methane and the iron atom suggests that this is the bond

Scheme IV

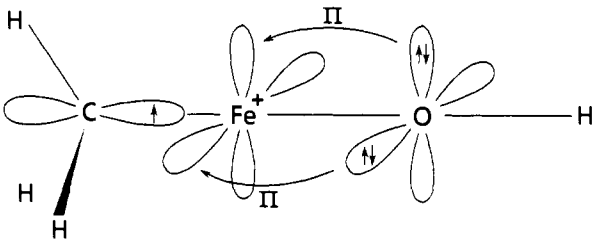

preferentially cleaved upon collisional activation. This is precisely borne out in the experiment.

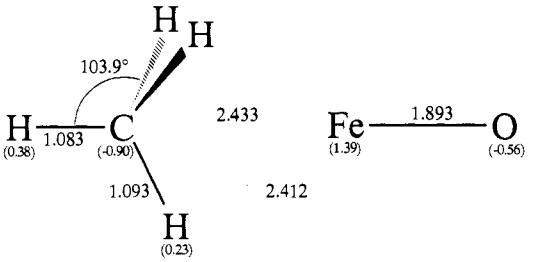

1

[- 12 kcal/mol]

As already mentioned, all attempts to transform computationally **1** to the complex **2**, which consists of CH_3· and $HFeO^+$ (or $FeOH^+$), failed; rather, full geometry optimization leads to the methyl iron hydroxide **3**. This ion, which formally corresponds to the insertion product of Fe^+ in the C–O bond of methanol, can be viewed as the result of a σ-metathesis[43] process between a CH bond of methane and the FeO bond, followed by structural relaxation to yield the C_{3v}-symmetric species **3**. The $\langle S^2 \rangle$ value of 8.75 is in accord with a relatively pure sextet state. The geometric features support that **3** can be described as a relatively unperturbed $FeOH^+$ species (d_{O-H} = 0.945 Å; d_{Fe-O} = 1.773 Å) interacting with a methyl radical. A quite long Fe–C bond length results (2.515 Å), and the FeCH bond angle is reduced to 97.6°. For an isolated $FeCH_3^+$ ion, we obtained the following structural data: d_{Fe-C} = 2.202 Å; d_{C-H} = 1.091 Å; ∠FeCH = 104.0°); a comparison of these data with the geometrical features of **3** underlines our interpretation. Also the electronic structure of the methyl subunit of **3** can be better described in terms of a slightly distorted sp^2-hybridized methyl radical, whose p_x orbital interacts with the $FeOH^+$ fragment. According to the spin density analysis of **3**, the unpaired electron is mainly located at the carbon atom. The linear arrangement of the HOFe unit of **3** results for the interaction of the unoccupied p_π orbitals of the methyl ion with both lone electron pairs of the oxygen atom. This leads to a significant deviation in the π system of Fe. Back-donation of electrons in the sp-hybrid orbital of the oxygen atom is used to form the σ_{OH} bond.[18] A pictorial description of the bonding is given in Scheme IV. The observed fragmentation pattern of system II is in keeping with structure **3**. It is the long Fe–C bond which is preferentially cleaved, resulting in the formation of $FeOH^+$ and CH_3·; although much less pronounced, the structure-indicative cleavage of the Fe–O bond to eventually generate OH· and $FeCH_x^+$ species (*x*

= 1–3) is also observed. The presence of a signal for Fe^+ in system II either results from reductive elimination of CH_3OH from **3**, or, alternatively, post-collisional isomerization **3** to the ion/methanol complex **4** cannot be ruled out. From a thermochemical point of view, **4** is significantly more stable than **3** (ca. 30 kcal/mol).

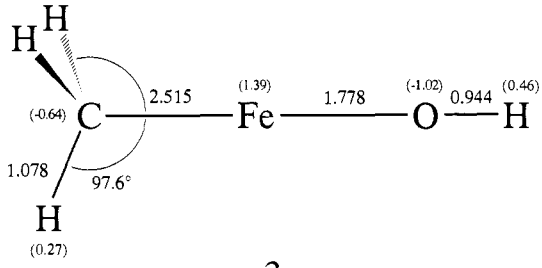

3

[- 35 kcal/mol]

The ECP-DZ calculations for **4** lead to a minimum with C_s symmetry; its ^6A state is only slightly spin-contaminated ($\langle S^2 \rangle$ = 8.752). We note the following structural features. Complexation of methanol by Fe^+ does not significantly alter the geometry of the organic part; only the C–O bond is elongated by 0.05 Å, while the C–H bonds remain unchanged. Interaction of the lone electron pair of oxygen with Fe^+ accounts for the Fe–O bond. The assignment of structure **4** to systems II and IV (Table III) is supported by the calculations, as the dominant fragmentation processes are expected to correspond to either the loss of the intact CH_3OH ligand or cleavage of the O–C bond to eventually generate the thermochemically attractive product combination $FeOH^+$ and $CH_3^{\bullet}$. Also, the nearly complete absence of any $FeCH_x^+$ fragments in the CA spectra of systems II and IV is in line with structure **4**.

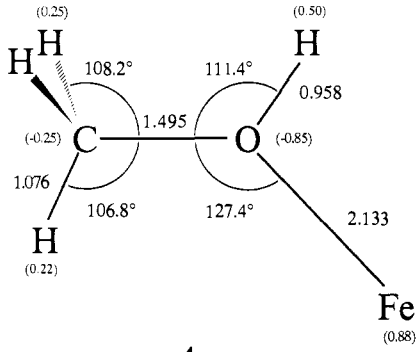

4

[-65 kcal/mol]

The aquo iron carbene complex $H_2C{=}Fe{-}OH_2^+$ (**7**), having C_{2v} symmetry and corresponding to a sextet state with $\langle S^2 \rangle$ = 8.78, is calculated to be the second most stable isomer on the potential energy surface of $[Fe,C,H_4,O]^+$ examined at the ECP-DZ level of theory (E = –60 kcal/mol, relative to separated FeO^+ and CH_4). The bond situation fits both the subunits $H_2C{-}Fe^+$ (**12**) and $Fe{-}OH_2^+$ (**13**), respectively, given below together with the structure of **7**. The calculated high stability of **7** is in agreement with previous experimental and theoretical data for $L{-}Fe{-}OH_2^+$ complexes (L = ligand); according to these observations[40] the introduction of a second ligand L causes an increase of the $Fe{-}OH_2^+$ bond energy. The fragmentation pattern of system I is in agreement with structure **7**; the CA spectrum (Table II) is dominated by an abundant H_2O loss process to generate $FeCH_2^+$ and products thereof ($FeCH_x^+$, x = 0–2). Cleavage of the FeC bond of **7** to generate CH_2 and $FeOH_2^+$ is, as expected from the thermochemical data (Table II) and in keeping with the bonding properties of **7**, less pronounced.

As mentioned in the Discussion section, we do not think to have experimental evidence that the formal insertion product of an Fe^+ ion in the O–H bond of methanol, i.e., $H_3CO{-}Fe{-}H^+$ (**8**), is generated as an observable species in the experiments reported here.[41] System IV ($HCOOCH_3$) upon Fe^+-mediated decarbonylation yields an $[Fe,C,H_4,O]^+$ ion whose CA spectrum is practically identical with that of the CH_3OH/Fe^+ complex **4**; in addition, the fragmentation pattern is indeed in keeping with structure **4**. Consequently, we argue that loss of CO from $HCOOCH_3/Fe^+$ also generates **4**. This, of course, does not imply that **8** is not a genuine minimum on the $[Fe,C,H_4,O]^+$ potential energy surface. In fact, the ECP-DZ calculations clearly demonstrate that the sextet state of **8** corresponds to a minimum ($\langle S^2 \rangle$ = 8.81), having C_s symmetry. The quasi-linear H–Fe–O–C unit of **8** ($\angle$H–Fe–O = 180.4°; $\angle$Fe–O–C = 180.2°) is of similar origin as already discussed for **3**. We note that both the H–Fe distance and the charge distribution of the HFe subunit of **8** are quite close to that reported for the $^5\Pi$ state of FeH^+.[26] As a consequence, it is no surprise that the geometrical features of the OCH_3 part of **8** are hardly altered when compared with an isolated methoxy radical.

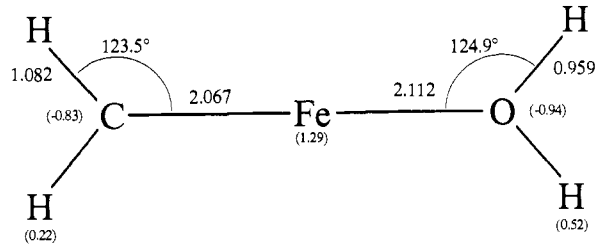

7

[- 60 kcal/mol]

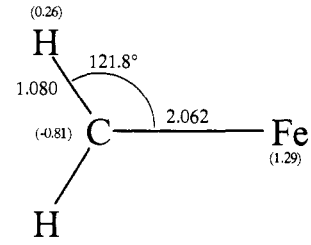

12

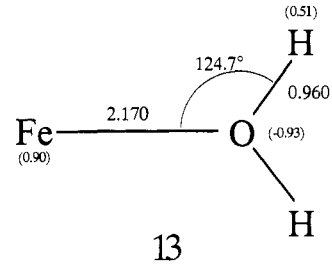

13

If **8** were indeed formed in the decarbonylation of $HCOOCH_3$ and would retain its structural integrity, one would predict a very intense signal for FeH^+ (loss of CH_3O) in the CA spectrum of system IV. This is not observed. Rather, the CA spectrum is dominated by loss of CH_3OH (to generate Fe^+), and the structure-indicative, though weak signal for $CH_3OH^{\bullet+}$ is also present. We therefore propose that **8** undergoes facile isomerization to the $CH_3O(H)Fe^+$ complex **4**. According to the calculations, this reaction is quite exothermic (–50 kcal/mol).

All attempts to locate the hydroxymethyl iron hydride **9** ($H{-}Fe{-}CH_2OH^+$) as a minimum of the $[Fe,C,H_4,O]^+$ sextet potential energy surface failed as, irrespective of the starting geometry, the optimization invariably resulted in the C_1-symmetric structure **14** ($\langle S^2 \rangle$ = 8.81). The geometry and the electronic structure of **14** are quite similar to those calculated for the linear $^4A'$ state of $H{-}Fe{-}OH^+$. For the latter, the relevant data are as follows: d_{H-Fe} = 1.68 Å, d_{Fe-O} = 2.189 Å, and d_{O-H} = 0.972 Å. For **14**

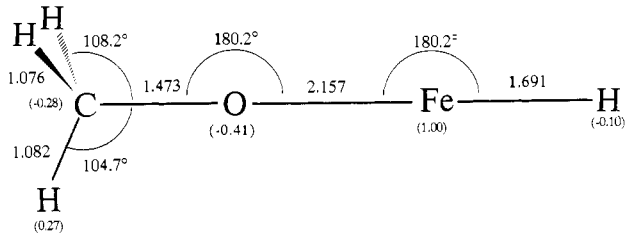

8

[- 15 kcal/mol]

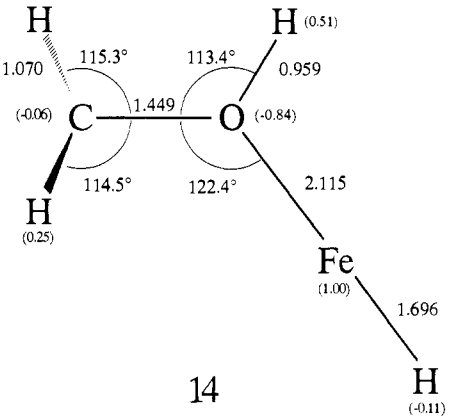

14

[- 12 kcal/mol]

one would expect that collisional activation inter alia gives rise to an abundant FeH^+ signal, this is not the case (Table III). Rather, the CA mass spectrum of system VII ($HCOCH_2OH$) can be explained by a 5:1 mixture of the two isomers **3** and **7** (H_3C–Fe–OH^+ and H_2C=Fe—OH_2^+, respectively). Obviously, quite a complex rearrangement of **14** to the thermochemically much more stable isomers **3** and **7** occurs by mechanisms which, for the time being, are not fully understood.

Finally, we would like to point out that the various $[Fe,C,H_4,O]^+$ isomers described in this section can be assigned to four different classes of bonding types. As indicated by the data given in Table V, while the d-electron population at the iron atom is almost unchanged for all isomers, we obtain quite pronounced differences for the s- and p-electron populations.

In complex **4** there is a clear σ-interaction from the doubly occupied orbital at the oxygen atom with the empty p_σ orbital of iron. The s-occupancy is unchanged.

For the isomers **8** and **14** we observe the same populations as for the H–Fe–OH^+ complex, which is given as a reference; here the ss- and sp-overlap lead to a lowering of the s-population and the donation of 0.18 electron in the p_σ of iron. In complexes **1** and **3**, the iron is formally oxidized, as ca. 0.8 electron from the s orbital is removed; a modest π-donation (ca. 0.1 electron) in the p_π orbital occurs.

The population of **7** differs from all bonding types considered. Donation in the π- as well as σ-system is observed. This is in accordance with both the Fe–O and Fe–C bond lengths of **7**.

Acknowledgment. We gratefully acknowledge financial support of our work by the Deutsche Forschungsgemeinschaft, Volkswagen-Stiftung, Fonds der Chemischen Industrie, and Gesellschaft von Freunden der Technischen Universität Berlin. Constructive comments and suggestions by the reviewers are appreciated.

Registry No. **3**, 138259-33-3; **4**, 138259-34-4; **7**, 138259-35-5; **8**, 138259-36-6; **12**, 90143-30-9; **13**, 126492-96-4; **14**, 138259-37-7; c-C_3H_6, 75-19-4; CH_3SO_2OH, 75-75-2; CH_3OH, 67-56-1; $HCOOCH_3$, 107-31-3; CH_4, 74-82-8; n-C_3H_7OH, 71-23-8; $HCOCH_2OH$, 141-46-8; CH_3COOH, 64-19-7; $Fe(CO)_5$, 13463-40-6; FeO^+, 12434-84-3.

Atomic Scale Imaging of Alkanethiolate Monolayers at Gold Surfaces with Atomic Force Microscopy

Carla A. Alves, Earl L. Smith, and Marc D. Porter*

Contribution from Ames Laboratory—U.S. Department of Energy and the Department of Chemistry, Iowa State University, Ames, Iowa 50011. *Received September 3, 1991*

Abstract: Monolayer films formed by the chemisorption of alkanethiols ($CH_3(CH_2)_nSH$, n = 1–17) at epitaxially grown Au(111) films were examined using atomic force microscopy (AFM). Atomically resolved images were found for films with $n \geq 4$, directly revealing for the first time the arrangement of the alkyl chain structure. All of the images exhibit a periodic hexagonal pattern of equivalent spacings (e.g., respective nearest- and next-nearest-neighbor distances of 0.52 ± 0.03 and 0.90 ± 0.04 nm for n = 17 and 0.51 ± 0.02 and 0.92 ± 0.06 nm for n = 5). These spacings agree well with the analogous 0.50- and 0.87-nm distances of a $(\sqrt{3} \times \sqrt{3})R30°$ adlayer on a Au(111) lattice, the two-dimensional arrangement reported in recent diffraction[1-3] and scanning tunneling microscopy[4,5] studies. In some instances, images with the above spacings were observed to extend continuously over areas as large as 100 nm^2, suggesting the potential of AFM to reveal both the short- and long-range order of the alkyl chains of these and other model interfacial structures. The implications of these findings, including the inability to obtain well-resolved images for films with $n \leq 3$, are examined in the context both of the current structural descriptions of alkanethiolate monolayers and of general issues related to imaging organic films with AFM.

Introduction

The atomic force microscope[6] (AFM) and its predecessor, the scanning tunneling microscope[7] (STM), have emerged as powerful tools for imaging semiconductor,[8] metallic,[9] organic,[10] and biological[11] surfaces with atomic scale resolution in environments ranging from ultrahigh vacuum to aqueous solutions. We have recently begun to assess the applicability of both techniques for imaging model organic interfacial systems, such as the alkanethiolate[12] monolayers that form on gold surfaces. The goal is to

* To whom correspondence should be addressed.

(1) Chidsey, C. E. D.; Liu, G.-Y.; Rowntree, P.; Scoles, G. *J. Chem. Phys.* **1989**, *91*, 4421–3.

(2) (a) Strong, L.; Whitesides, G. M. *Langmuir* **1988**, *4*, 546–58. (b) For additional details: Chidsey, C. E. D.; Loiacono, D. M. *Langmuir* **1990**, *6*, 682–91.

(3) Samant, M. G.; Brown, C. A.; Gordon, J. G., II. *Langmuir* **1991**, *7*, 437–9.

0002-7863/92/1514-1222$03.00/0